# Prospect of new ocean waves spectral observations from the SWIMSAT satellite: measurements and assimilation

**Danièle Hauser**

*CETP/CNRS/Université de Versailles Saint-Quentin*
*10-12 Avenue de l'Europe, F-7140 Vélizy, France,* hauser@cetp.ipslfr

**Lotfi Aouf and Jean-Michel Lefevre**

*Météo-France, Marine Forecast Service*
*42 Avenue G. Coriolis, F-31057 Toulouse Cedex, France*

**Abstract**

The project SWIMSAT (Surface Waves Investigation and Monitoring from SATellite) aims to measure the directional spectra of waves from space using a real-aperture radar with a low-incidence beam (0-10°) scanning in azimuth (0-360°). In this paper we present the instrument principle and the proposed mission. The performance in terms of wave spectra measurement has been estimated by taking into account the various sources of uncertainties. The simulations show that in the chosen configuration, SWIMSAT is capable of measuring wave spectral properties in wind-sea conditions (at dominant wavelengths over approximately 70 meters) and swell conditions (at significant wave heights over approximately 1.5 to 2 meters, depending on wind). Unlike for SAR observations, the inversion of SWIMSAT data does not require any a priori knowledge of the wind-sea part and the minimum detectable wavelength is independent on the wave propagation direction. Preliminary results of an assimilation study, using synthetic SWIMSAT data, are also presented here below. They show that the predicted wave parameters tend to the observed data, and then significantly improve the estimation of the wave height.

## 1. Introduction

Today, most operational meteorology centers use numerical models to provide ocean wave predictions. Unlike atmospheric circulation models, it is only recently that assimilation of observations are used in these models to constraint the solution. Furthermore, data assimilation in wave prediction models is presently mainly based upon observations of the total energy (or significant wave height) of the wave spectrum, ignoring their spectral properties (Janssen et al., 1989, Lionello et al., 1992, Breivik and Reistad, 1994, Mastenbroek et al., 1994). In these studies, radar altimeter data of significant wave heights are commonly used. The main drawback of these methods, based on the assimilation of total energy alone, is that they need certain assumptions about the characteristics of the wave field, and in particular the separation between swell and wind-sea. This might generate errors or reduce the impact of the assimilation. Recent studies (De La Heras et al., 1994, Voorrips et al., 1997, Breivik et al., 1998) have proved the interest of assimilation of spectral information, although these studies concern small geographical zones (e.g. part of the North Sea or Norwegian Sea). They show that to improve numerical wave predictions, spectral information is necessary to decrease errors either due to the model itself (parameterizations, numerical uncertainties) or to the forcing surface wind field. For ocean-basin predictions, only satellite data can provide observations compatible with the large-scale forecast.

Synthetic aperture radar (SAR) is currently the only technology for estimating directional ocean wave properties from a sensor. But SAR has one major drawback: it is now well known that the wave-like patterns

visible in SAR images of the ocean surface may be considerably different from the actual ocean wave field. As a result, extracting meaningful two-dimensional wave spectral properties from a SAR scene is not straightforward. The SAR's ability to provide usable ocean wave spectra is limited by the motion of the ocean surface. Doppler misregistrations in azimuth (along-track) are induced by motions of the scatters, leading to a distortion of the imaged spectrum and a strong cut-off in the azimuth direction. This non-linear effect is proportional to the range-to-velocity ratio of the platform. For present and future missions (ERS, Radarsat, Envisat) this ratio is high (about 120 s), leading to minimum detectable wavelengths of about 150 to 200 m for waves propagating in the along-track direction. Furthermore, the non-linearity of the relation between image spectrum and wave spectrum requires the use of quite complicated algorithm in which the wind-sea part must be specified. Until recently, the whole wave spectrum was specified from wave prediction models as a first guess of an inversion iterative procedure (Hasselmann and Hasselmann, 1991, Brüning et al, 1994, Engen and Johnsen, 1994, Hasselmann et al 1996, Heimbach et al, 1998, among others). This led to some controversy about the independence of SAR-inverted data from models.

More recently, significant progress has been accomplished in the use of SAR data, in particular in the context of the preparation of the ENVISAT mission (Engen and Johnsen, 1995, Mastenbroek and De Valk, 2000). Wave model information is no longer required to remove the 180° ambiguity in the propagation direction and external wind information (from scatterometer observations, model wind fields or from the SAR radar cross-section) can be used to extract the directional properties of the long-wave part of the spectrum. These new improvements need still to be validated with the future ENVISAT observations. Anyway, it is clear that no wave information will be extracted from the SAR for wavelengths less than the cut-off limit. This cutoff-limit depends on wind and wave conditions and is typically 150-200 m for waves travelling in the azimuth direction. In addition, the uncertainties in the wind-sea part which must be fixed in the inversion, are still a limiting factor.

To fill this gap, the SWIMSAT concept (Hauser et al, 2001) has been proposed. It is based on the use of a space-borne real-aperture radar (RAR) system, instead of a SAR. A preliminary definition of the radar was proposed in Hauser et al (2001). It was based on a dual-beam Ku-band radar (nadir viewing and off-nadir viewing at an angle of 10°) and scanning in azimuth over 360°. Work is under progress to define a new version, with a radar beam scanning both in incidence (0-10°) and in azimuth (0-360°). This would permit to obtain the directional spectra at a scale of about 50 km x 50 km, and also to estimate the wind speed at the same scale. This concept will be submitted in response to the call for opportunity missions of the "Earth Explorer" Program issued by the European Space Agency in 2001.

In section 2 we present the measurement principle on which the retrieval of the directional spectrum is based. Section 3 presents the main features of the proposed SWIMSAT mission and instrument. Section 4 summarizes the expected performance of the directional wave spectrum measurement. Preliminary studies have been performed on assimilation of SWIMSAT data into a wave prediction model. They are summarized in Section 5.

## 2. SWIMSAT: measurement principle

The measurement principle has been well documented in the literature (Jackson et al 1981, Jackson et al 1985a-b, Jackson and Lyzenga, 1990, Hauser et al, 1992). Here, we focus our attention on the main features of this principle only.

At low incidence, the backscattering mechanism is dominated by quasi-specular reflection from facets oriented perpendicular to the radar look direction. Facets with wavelengths larger than three to five times the electromagnetic wavelength contribute to this process. The normalized radar-cross section $\sigma_0$ is related to the probability density function of the short waves forced by the wind stress. This normalized radar-cross section is modulated by the local slope of the surface due to the long waves. This is the so-called "tilt modulation". The tilt modulation can be considered dominant and linear under the following conditions:

i) long-wave slope is small (less than 10%), which is a reasonable assumption for standard ocean waves;

ii) hydrodynamic modulation is negligible; this process has been described extensively (Alpers et al, 1981) as a hydrodynamic effect that modulates the energy density of the capillary-Bragg waves along the long-wave profile. Near 10° incidence angle, the backscatter intensity is almost independent upon roughness because the reflection conditions are intermediate between specular (where the backscatter intensity decreases with roughness) and Bragg (where the backscatter intensity increases with roughness).

iii) the footprint in the azimuth direction ($L_y$) is large with respect to the correlation length of the surface in the same direction; this assumption is valid when $L_y$ is larger than the longer waves to be analyzed.

It is recognized (Jackson et al, 1985 a,b, Hauser et al, 1992) that in this configuration (low incidence angle, large footprint with respect to the wavelength of the waves to be measured), the density spectrum of the modulation of the backscattered signal $P_m(k,\phi)$ is linearly related to the slope spectrum $k^2F(k,\phi)$ of the waves, for wavelengths larger than about 40 m:

$$P_m(k,\phi) = \frac{\sqrt{2\pi}}{L_y}\alpha^2 k^2 F(k,\phi) \tag{1}$$

where $L_y$ is the width of the footprint in the azimuth direction, k is the wavenumber of the waves, $\phi$ their traveling direction, and $\alpha$ is related to the fall-off of the normalized radar cross-section $\sigma_0$ with incidence angle $\theta$:

$$\alpha = cotg\,\theta - \frac{1}{\sigma_0}\frac{\partial \sigma_0}{\partial \theta} \tag{2}$$

In $\alpha$, the derivative of $\sigma_0$ is dependent on the mean square slope of the surface; i.e. mainly wind-conditions. It must be estimated for each spectrum. Several methods can be used to achieve this. The first one, developed and used for processing airborne RESSAC data (Hauser et al, 1992), consists of calculating $\alpha$ using the measured $\sigma_0$ values as a function of incidence angle $\theta$. An alternative method is to estimate $\alpha$ by normalizing the $P_m$ values using an independent measurement of the significant wave height $H_s$, where $H_s$ is related to the wave spectrum by:

$$H_s = 4\sqrt{\iint F(k,\phi)dkd\phi} \tag{3a}$$

The nadir-beam of SWIMSAT will measure $H_s$ in the same way as for space-borne altimeters (see section 3). The value $\alpha$ can then by obtained through:

$$\alpha^2(\theta) = \frac{L_y}{\sqrt{2\pi}}\left(\frac{4}{H_s}\right)^2 \iint \frac{P_m(k,\phi)}{k^2} kdkd\phi \tag{3b}$$

If there are no perturbing noise sources, the wave-height spectrum $F(k,\phi)$ in the look direction $\phi$ can be inverted from the modulation spectrum $P_m(k,\phi)$ using Equation (1). To retrieve the full spectral information over all directions, a set of directions $\phi$ are sampled using a conical scan of the radar beam. Due to the fact that the radar measurements is related to the tilt of the waves which are nearly symmetric with respect to their crest, the directional wave spectra are obtained with an 180° ambiguity in the direction of propagation. Of course, noise sources must be taken into account both when dimensioning the system and in the post-processing. We will discuss these points in section 4.

## 3. Main features of the SWIMSAT mission and instrument

The proposed system for SWIMSAT is a radar operating in the Ku frequency band (13.565 GHz) and flying on a polar-orbiting satellite at an altitude of 450 to 600 kilometers (Figure 1). In the version proposed by Hauser et al (2001), a dual-beam system is used, one pointing towards nadir, the other one at 10° from nadir. The nadir-beam is designed to measure significant wave height and wind speed in the same way as spaceborne altimeters. The off-nadir viewing mode is designed to measure wave spectral characteristics, following the principle recalled here-above. The beam-aperture of the radar is 2 x 2 ° leading to a footprint of about 18 km radius. To acquire measurements in all directions of wave propagation, the beam is rotated to perform a conical scan around the vertical axis (Fig.1). This beam scanning is obtained by using an offset parabolic antenna, rotating only the feed horn, while keeping fixed the parabole.

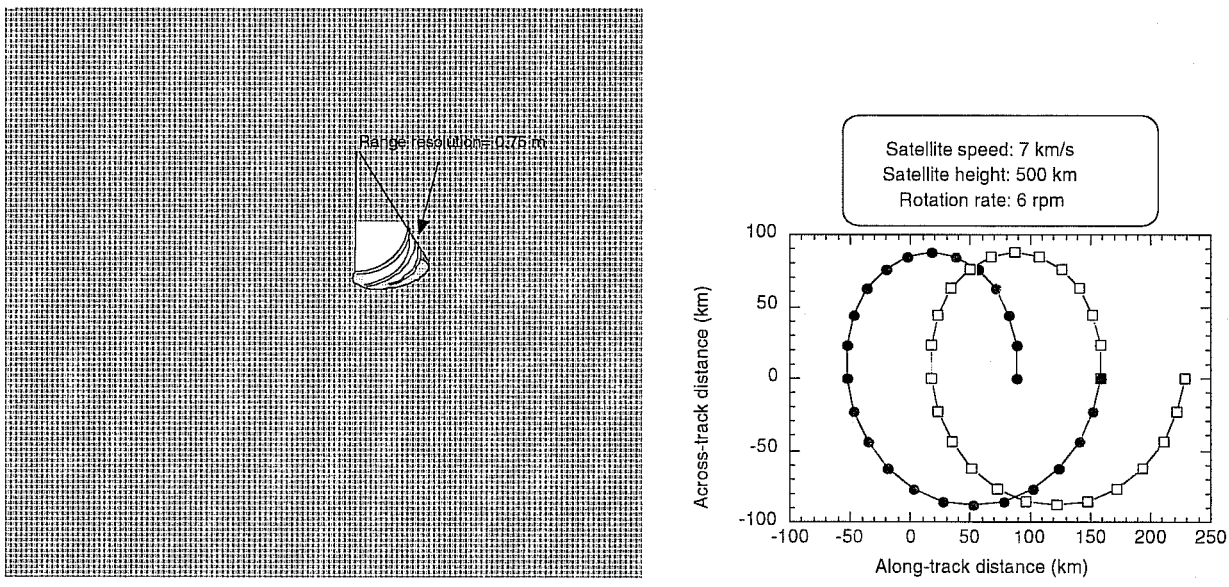


*Figure 1: Geometry of SWIMSAT in the option of a twin-beam antenna. Left part: geometry of the nadir and tilted beam (incidence 10°). Right part: horizontal pattern described by the 10° incidence beam.*

Improvement of this design is presently under study. It consists in a simultaneous electronic sweep in both incidence (0 to 10°) and azimuth (0 to 360°). The surface pattern described by the antenna in this condition is shown in Figure 2 for incidence angles every 2° from 6 to 10°. At a mean altitude of 500 kilometers the swath covered by a 360° scan has a radius of 52 to 88 km in radius, for incidence angles from 6 to 10°. This is compatible with the resolution offered by global wave prediction models (presently of the order of 0.5° x 0.5° to 1° x 1° in latitude-longitude). This altitude also ensures that the power budget is compatible with

measurement constraints. Table 1 presents the main characteristics of the radar itself, for the two-beam configuration (0 and 10° incidence).

| | **Nadir beam** | **Off-nadir beam** |
|---|---|---|
| Incidence | 0° | 10° |
| | **Microwave Part** | |
| Frequency | 13.575 GHz | 13.575 GHz |
| Peak RF power | 5 Watt | 50 to 100 Watt |
| Waveform | Chirp (frequency modulated) | Chirp (frequency modulated) |
| Bandwidth | 320 MHz | 200 MHz |
| Pulse duration | 80 µs | 50 µs |
| Pulse Repetition Interval | 500 µs | 250 µs |
| | **Antenna** | |
| Polarisation | VV | HH |
| 3 dB beamwidth | 2° x 2° | 2°x 2° |
| Rotation | 6 rotations/minute | 6 rotations/minute |
| | **On-board processing** | |
| Range Compression | full-deramp technique | numerical technique |
| Range resolution after compression | 0.47 m | 0.75 m |
| Time-integration | 50 ms<br>with correction of the advection using tracking-loop | 37 ms<br>with correction of the footprint displacement during time-integration |
| Space averaging | | 6 consecutive range gates |
| Level 1 processing | real time processing of distance, radar cross-section and significant wave height (MLE estimator) | real- time processing:of the modulation spectrum and averaging of this spectrum |

***Table 1:*** *Main characteristics of the radar for SWIMSAT in the two-beam configuration*

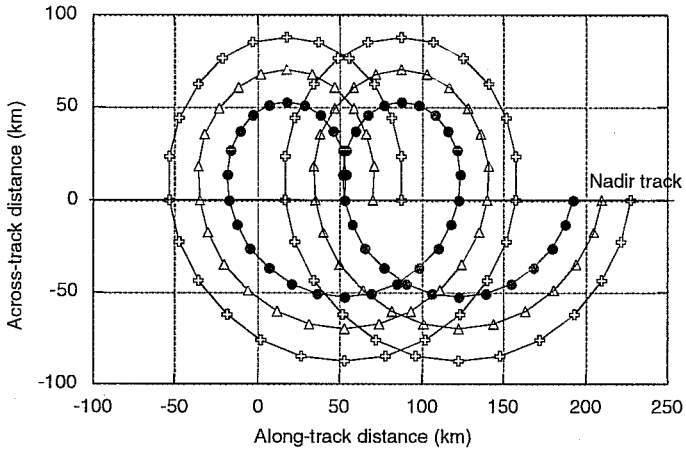


*Figure 2: Horizontal pattern obtained when combining three incidence angles (from 6 to 10°). The scale at which the full directional spectral information is obtained is 46 x 52 km (for 6° incidence), 50 x 70 km (for the 8° incidence) and 50 x 90 km (for the 10° incidence).*

## 4. Products and expected performance for the directional wave spectra measurement

From simulations (see Hauser et al, 2001), we studied the effect of the thermal signal-to-noise ratio and of the speckle noise. These simulations were based on a synthetic wavy surface calculated for a specified wave spectrum. The reference for these simulations were obtained by applying directly the linear model of Eq.(1) and an empirical $\alpha$ value. The radar measurement was simulated by taking into account thermal noise, speckle noise, and footprint displacement during the acquisition time. Inversion of this synthetic measurement was then performed in different conditions, in particular with and without ignoring speckle and thermal noise. It was shown that thermal noise is an important dimensioning factor. The transmitting power of the radar (100 W) was chosen in order to minimize errors due to this. We have also shown from simulations that speckle imposes a detection threshold and introduces a bias in the estimate of the modulation spectrum due to waves. However it is possible to minimize this speckle effect, by maximizing the radar's inherent resolution (here chosen to 0.75 m) and the number of independent samples, $N_{int}$, (product of the integration time $T_{int}$ and the pulse repetition frequency). However, integration time $T_{int}$ is also is constrained by the required effective horizontal resolution $\Delta X$ (Jackson et al., 1987), which is in turn limited by the curvature of the electromagnetic wavefront and the displacement due to the satellite's motion and antenna rotation of the horizontal sampled bins. The result of this trade-off is described in Table 1, both in terms of instrument definition and processing parameters.

In the processing of SWIMSAT data, both the thermal noise and speckle noise will be taken into account (see Hauser et al, 2001 for details). Thermal noise corrections can be applied by estimating the noise level from appropriate radar sequences and correcting the received power. The effect of speckle noise can be accounted for using the following equation:

$$Pm(k) \approx Pc(k) + Ps(k) \qquad (4)$$

where $P_m(k)$ is the measured spectral energy of the backscatter modulation, $P_c$ is the modulation spectrum which would be observed in absence of speckle and $P_s(k)$ is the spectral energy density of speckle. This latter is given by:

$$P_s(k) = \frac{1}{N_{\text{int}}\sqrt{2\pi}} \cdot \frac{\Delta x}{2\sqrt{2\ln 2}} \tag{5}$$

where $N_{int}$ in the number of independent samples (of the order of 150 for SWIMSAT) and $\Delta x$ is the intrinsic horizontal resolution (0.75 m).

Using the individual estimates of $F(k,\phi)$ (obtained typically within azimuth bins of the order of 1°) an averaging procedure must be applied to increase the number of degrees of freedom and decrease the statistical uncertainty. The final product for $F(k,\phi)$ will be calculated with a 15° azimuth sampling and for wavelengths from about 50 to 500 m.

Figure 3 illustrates the expected performance for a fully-developed wind sea case following a Pierson-Moskowitz shape (with a 13 m/s wind speed) and for a swell case (Hs= 4 m peak wavelength $\lambda_{peak}$=200 m, 13 m/s wind-speed). These results show the inverted radial spectrum $P_c(k)$ when the radar look direction is aligned with the wave propagation direction. The full solid line shows the reference. The line with symbol correspond to the inverted product, after averaging over 16 individual estimates (covering a 15° azimuth range), and where correction of thermal noise and speckle noise have been taken into account. The heavy horizontal line shows the speckle noise level. This shows that both the shape and the level of the spectrum can be correctly retrieved.

Concerning the absolute value of the wave spectrum, an estimate of $\alpha$ is necessary. If we keep the initial configuration of SWIMSAT (dual beam at 0 and 10° incidence), it will not be possible to estimate the $\alpha$ parameter of Eq.(1) using Eq.(2), because the term $\partial\sigma_0/\partial\theta$ will not be available. In this case, we will estimate $\alpha$ from Eq.(3), assuming an homogeneous wave energy at the scale of the swath (88 km radius). If the second option is chosen (simultaneous scan in azimuth and incidence from 0 to 10°), then $\alpha$ can be estimated from Eq.(2), assuming constant wind properties at the scale of the swath corresponding to each incidence (52 to 88 km in radius for incidence between 6 and 10°). This second option will also be tentatively used to estimate wind speed, since $\alpha$ is a function of wind speed.

In summary, from the simulation study, we could show that SWIMSAT should be capable of measuring wave spectral properties :

- under wind-sea condition, provided the dominant wavelength is greater than about 70 m,
- in swell conditions, provided the significant wave height is greater than 1.5 to 2 meters, depending on wind.

We have also shown that provided that an averaging process is applied, the inversion process would give an accuracy of about 20% in wave energy (10% in wave height). Resolution in direction is 15° after the averaging process is applied, whereas resolution in wavelength is about 20% of the wavelength. Due to the sampling variability, determination of the peak of the spectrum is subject to some uncertainty (see Fig3). Some smoothing process will be necessary to automatically extract the peak wavelength, but the accuracy in the estimate of the peak should be of the order of the wavelength resolution. The horizontal scale at which the complete 2D spectrum will be provided depends on the option that will be chosen. With incidence angles

covering from 6 to 10°, this scale can reach about 46 km (along-track) by 52 km (across-track), by combining successive rotation patterns as shown in Fig.2. If incidence angles are restricted to the two-beam configuration (0 and 10°) this scale would reach about 50 km (along-track) by 88 km (across-tack)

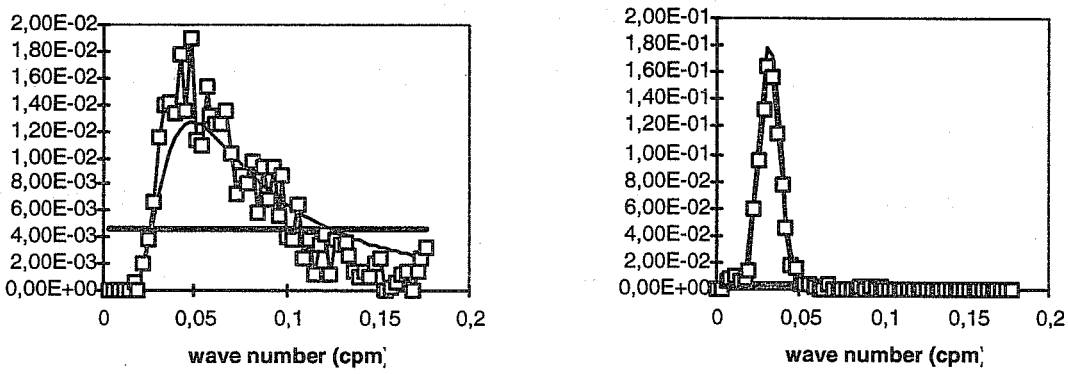


*Figure 3: Modulation spectra for a look direction aligned with the wave propagation direction (lines with square symbols). Left plot: Pierson-Moskowitz spectrum at a wind speed U=13 m/s. Right plot: swell spectrum with $H_s$=4m, $\lambda_{peak}$=200 m, U=13 m/s. Thin line without symbols: reference spectrum. Solid line with symbols: simulated SWIMSAT product, after correction of thermal and speckled noises. Heavy horizontal line: Speckle noise level.*

## 5. Assimilation of SWIMSAT data in wave prediction models

The proposed data for directional wave spectrum in the SWIMSAT project can be very helpful to improve wave prediction by numerical models. In this study we developed a simulation to analyse the impact of the assimilation of directional wave spectrum on the sea-state prediction. We used the wave model WAM cycle 4 implemented for the global scale 1x1 degrees in latitude and in longitude. The wave spectrum is discretisized in 24 directions and 25 frequencies ranging from 0.04 to 0.41 Hz, corresponding to the data given by the SWIMSAT. The assimilation code is based on the work of Vooripps et al. (1997) and uses the partitioning concept and an optimal interpolation on the integrated wave parameters, which are mean wave energy, mean wave frequency and mean wave direction. We recall that the partitioning concept consists to decomposes the wave spectrum in partitions which describe different wave systems corresponding to different meteorological events (wind-sea, swell or combined sea). The correlation model used in the optimal interpolation is of an exponential form depending on the distance between the locations and the correlation length, which is taken equal to 200 km, while the influence radius characterizing the area of impact is of 1000 km.

More than 600 observation locations are used in this study and followed an ERS-1 track. The simulation consists at first to run the wave model without assimilation and with an analysed ECMWF wind fields as wind input. The obtained directional wave spectra at the observation locations will be considered as a synthetic SWIMSAT data. Secondly the wind fields are disturbed to make a small change of the wave field and the wave model is run with the assimilation of synthetic data to correct this latter. We proposed two different ways to disturb the wind input. The first one is to consider a shift of 12 hours of the analysed wind field. The second one is to use forecasted wind fields (6 and 12 hours range) from the atmospheric model. A period is selected for the assimilation test starting from October 22, 2000. The data is assimilated every 6 hours during the first day and after that, the assimilation is stopped and the effect in time is analysed.

Figure 4 shows the impact of the assimilation on the significant wave height: we can see that the difference can reach locally more than 2 m. The impact gradually decreases with time but remains significant up to 3 days as illustrated in figure 5, where the difference is less than 0.1 m. Other tests also show that when we increase the period of assimilation and the number of data, the impact in time is longer. To analyse the effect of directional parameters in the assimilation we just assimilated the altimeter data in the wave model. Figure 6 shows that the wave height is smaller of more than 1 m comparing to the case including directional parameters. Statistical analysis on other results is under development. Further, the dependence between the code performance and the threshold distance in wavelength space which characterize the cross-assignement between first-guess and observed wave systems, will be studied and presented in future. To complete this study, measurement errors or limitations associated with the SWIMSAT system will be introduced in the assimilation study. In addition this type of simulation, will be used to optimize the sampling proposed for the SWIMSAT mission.

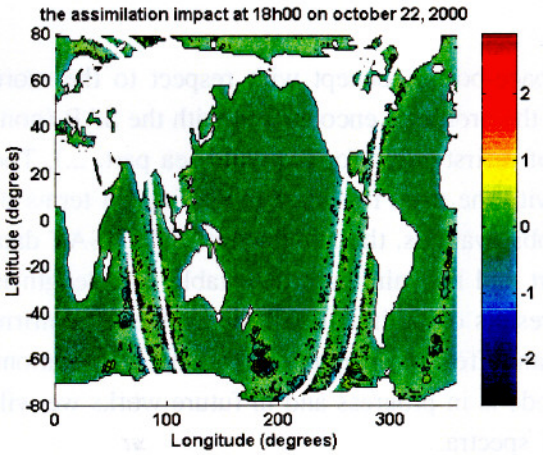


*Figure 4: Difference in meters of significant wave heights before and after assimilation of the synthetic SWIMSAT data; the white line shows the locations of the observations. In this case, the simulated wave field before assimilation was generated by running the WAM model forced by wind fields from the forecast instead of winds from the analysis.*

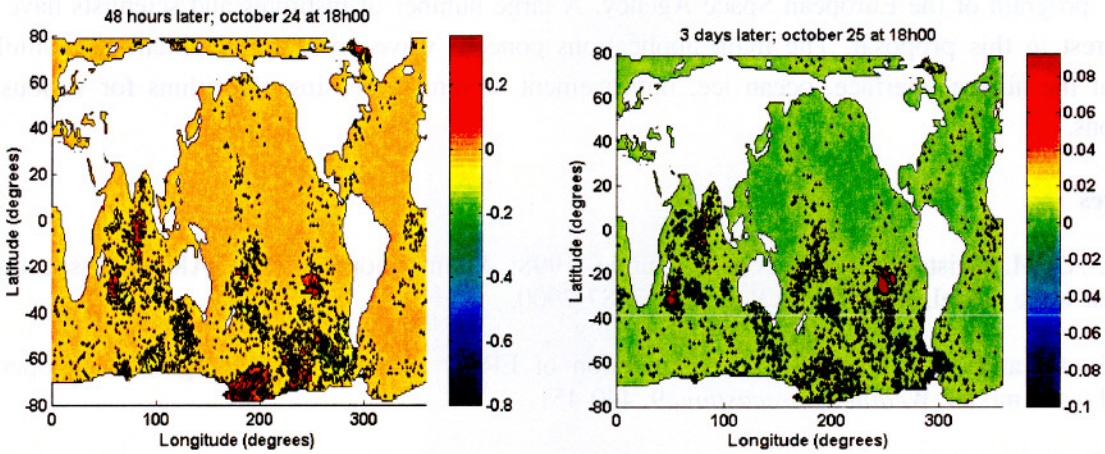


*Figure 5: Difference in meters of significant wave heights between model run with and without assimilation; (left plot) : 48 hours and (right plot) 3 days after the assimilation time. Same conditions for the simulation as in Figure 4.*

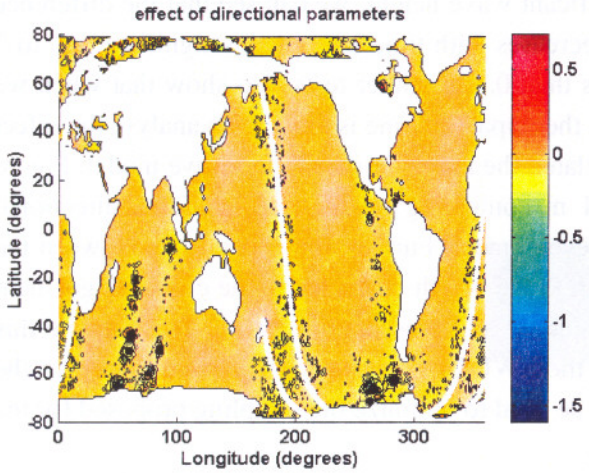


*Figure 6: Difference in meters of significant wave heights between model run with and without directional parameters; white line shows the data locations. Same conditions for the simulation, as in Figure 4.*

## 6. Conclusion

The SWIMSAT concept has been presented. It is a new space-borne concept with respect to the more classical SAR missions. This concept should alleviate most of the problems encountered with the SAR (non-linear relation between SAR image and wave image, needs of a first-guess for the wind-sea part, ...). The expected performances of SWIMSAT are quite compatible with the need for wave modelling, in terms of scale and type of parameters and accuracy. Unlike for SAR observations, the inversion of SWIMSAT data does not require any a priori knowledge of the wind-sea part and the minimum detectable wavelength is independent on the wave propagation direction. Preliminary results on assimilation in wave model confirm the improvement of the wave prediction and show the significant effect of using the directional informations of the wave spectrum. The optimisation of the assimilation code is in progress and in future works we will take into account a SWIMSAT track and simulated SWIMSAT spectra.

The SWIMSAT project will be submitted at the end of 2001, as a proposal in the context of the "Earth Explorer" program of the European Space Agency. A large number of institutes and scientists have shown their interest in this proposal. The main applications concern wave prediction (validation, assimilation), physics of the air/sea interface, ocean ice, improvement of remote sensing algorithms for various ocean applications.

### References

Breivik L-A., M. Reistad, H. Schyberg, J. Sunde, 1998: Assimilation of ERS SAR wave spectra in an operational wave model, *J. Geophys. Res.*, **103**, 7887-7900.

Breivik, L.-A., and M. Reistad, 1994: Assimilation of ERS-1 altimeter wave heights in an operational numerical wave model, *Weather Forecasting*, **9**, 440-451.

Brüning C., S. Hasselmann, K. Hasselmann, S. Lehner, and T. Gerling, 1994: A first evaluation of ERS-1 synthetic aperture radar wave mode data, *The Global Atmos. and Ocean Syst.*, **2**, 61-98.

De La Heras M. M., G. Burgers, and P.A.E.M. Janssen,1994: Variational wave data assimilation in a third-generation wave model, *J. Atmos. and Oceanic Tech.*, **11**, 1360-1369.

Engen G., and H. Johnsen, 1994: Directional wave spectra by inversion of ERS-1 synthetic aperture radar ocean imagery, *IEEE Trans. on Geoscience and Remote Sensing*, **32**, 340-352.

Engen G., and H. Johsen, 1995I: SAR-Ocean wave inversion using image cross-spectra, *IEEE Trans. On Geoscience and Remote Sensing*, **33**, 1047-1056.

Hasselmann K.and Hasselmann S., 1991: On the non-linear mapping of ocean wave spectrum into a SAR image spectrum and its inversion, *J. Geophys Res.*, **96**, 10,713-107129.

Hasselmann S., C. Brüning, K. Hasselmann, and P. Heimbach, 1996: An improved algorithm for the retrieval of ocean wave spectra from synthetic aperture radar image spectra, *J. Geophys. Res.*, **101**, 15, 615-16, 629.

Hauser D., E. Soussi, E.,Thouvenot, L. Rey, 2001: SWIMSAT: A real aperture radar to measure directional spectra of ocean waves from space, Main characteristics and performance simulation, *J. Atmos. and Oceanic Tech*, **18**, 421-437.

Hauser D., G. Caudal, G.J. Rijckenberg, D. Vidal-Madjar, G. Laurent, P. Lancelin, 1992: A new airborne FM/CW radar ocean wave spectrometer, *IEEE Trans on Geoscience and Remote Sensing*, **30**, 981-995.

Heimbach, P., S. Hasselmann, and K. Hasselmann, 1998: Statistical analysis and WAM model intercomparison of wave spectral retrievals for a 3 year period of global ERS-1 SAR wave mode, *J. Geophys. Res.*, **103**, 7931-7978.

Jackson F. C., 1981: An analysis of short pulse and dual frequency radar techniques for measuring ocean wave spectra from satellites, *Radio Science*, **16**, 1385-1400.

Jackson F. C., T.W. Walton., P.L. Baker, 1985a: Aircraft and satellite measurement of ocean wave directional spectra using scanning-beam microwave radars, *J. Geophys. Res.*, **90**, 987-1004.

Jackson F. C., W.T.Walton, and C.Y. Peng, 1985b: A comparison of in situ and airborne radar observations of ocean wave directionality, *J. Geophys. Res*, **90**, 1005-1018.

Jackson F.C, 1987: The Radar Ocean-Wave Spectrometer, *Johns Hopkins APL Technical Digest*, **8**, 116-127.

Jackson F.C., and D.R. Lyzenga, 1990: Microwave techniques for measuring directional wave spectra, In: *Surface Waves and Fluxes, Vol. II,* eds. G.L. Geenaert and Plant W.J., Academic Press, 221-264.

Janssen P.A.E.M., P. Lionello, M. Reistad, and A. Hollingsworth, 1989: Hindcasts and data assimilation studies with the WAM model during the SEASAT period, *J. Geophys. Res.*, **94**, 973-993.

Lionello P., and H. Günther, 1992: Assimilation of altimeter data in a global third-generation model, J. *Geophys. Res.*, **97**, 14,453-14,474.

Mastenbroek C., and C.F. De Valk, 2000: A semi-parametric algorithm to retrieve ocean wave spectra from SAR, *J. Geophys. Res*, **105**, 3497-3516.

Mastenbroek C., V.K. Makin, A.C. Voorrips, and G.J. Komen, 1994: Validation of ERS-1 altimeter wave height measurements and assimilation in a North Sea wave model, the Global Atmos. *Ocean Syst*, **2**, 163-184.

Voorrips A.C., V.K. Makin, and S. Hasselmann, 1997: Assimilation of wave spectra from pitch-and-roll buoys in a North Sea wave model, *J. Geophys. Res.*, **102**, 5829-5849.